CHAPTER EIGHT

THE INFLUENCE OF DETECTOR SIZE RELATIVE TO FIELD SIZE IN SMALL-FIELD PHOTON-BEAM DOSIMETRY USING SYNTHETIC DIAMOND CRYSTALS AS SENSORS

Submitted in March 2014 to Radiation Physics and Chemistry

The influence of detector size relative to field size in small-field photon-beam dosimetry using synthetic diamond crystals as sensors

N. Ade and T.L. Nam[+]

School of Physics, Radiation and Health Physics Unit and DST-NRF Centre of Excellence in Strong Materials, University of the Witwatersrand, Private Bag 3, Wits 2050, Johannesburg, South Africa.

Abstract

The choice of a detector for small-field dosimetry remains a challenge due to the size/volume effect of detectors in small fields. Aimed at selecting a suitable crystal type and detector size for small-field dosimetry, this study investigates the relationship between detector and field size by analysing output factors (OFs) measured with a Diode E (reference detector), a Farmer chamber and synthetic diamond detectors of various types and sizes in the dosimetry of a 6 MV photon beam with small fields between 0.3x0.3 cm^2 and 10x10 cm^2. The examined diamond sensors included two HPHT samples (HP1 and HP2) and six polycrystalline CVD specimens of optical grade (OG) and detector grade (DG) qualities with sizes between 0.3 and 1.0 cm. Each diamond was encapsulated in a tissue-equivalent probe housing which can hold crystals of various dimensions up to 1.0x1.0x0.1 cm^3 and has different exposure geometries ('edge-on' and 'flat-on') for impinging radiation. The HPHT samples were found to show an overall better performance compared to the CVD crystals with the 'edge-on' orientation being a preferred geometry for OF measurement especially for very small fields. For instance, down to a 0.4x0.4 cm^2 field a maximum deviation of 1.9% was observed between the OFs measured with Diode E and HP2 in the 'edge-on' orientation compared to a 4.6% deviation in the 'flat-on' geometry. It was observed that for fields below 4x4 cm^2, the dose deviation between the OFs measured with the detectors and Diode E increases with increasing detector size. It was estimated from an established relationship between the dose deviation and the ratio of detector size to field size for the detectors that the dose deviation probably due to the volume averaging effect would be > 3% when the detector size is > 3/4 of the field size. A sensitivity value of 223 nC Gy^{-1} mm^{-3} was determined in a 0.5x0.5 cm^2 field with HP2 compared to a value of 159.2 nC Gy^{-1} mm^{-3} obtained with the diode. The results of this study indicate that with careful selection of a suitable crystal type of a given size and orientation the relative dose measured with the diamond probe in small fields would agree favourably within ±2% with that measured with a small-field detector but with a higher sensitivity value.

Keywords: Synthetic diamonds, Small fields, Output factor, Detector size, Volume effect

[+] Corresponding author: Tel. +27 11 717 6878; +27 11 351 7001.
E-mail address: Tom.Nam@wits.ac.za

1. Introduction

Advanced techniques in external beam radiotherapy such as intensity modulated radiation therapy (IMRT), stereotactic radiosurgery (SRS), image guided radiation therapy (IGRT) and tomotherapy make use of small radiation fields (Zhu, 2010) in order to spare normal healthy tissues while high doses can be delivered to tumour volumes (Barnett et al., 2005; Das, 2009; Marsolat et al., 2013). Small fields are often used to treat conditions such as benign and malignant, intra and extra-cranial tumours (Marsolat et al., 2013). Small-field dosimetry is well known to be challenging due to a number of factors such as the tissue-equivalence of detectors, the loss or lack of lateral electronic equilibrium and the volume averaging effect of detectors in small fields (Haryanto et al., 2002; Laub and Wong, 2003; Das, 2009; Lee et al., 2012). The aspects of tissue-equivalence and volume effect have been noted to be both related to the absence of electronic equilibrium (Haryanto et al., 2002).

It is known that the equilibrium of secondary electrons breaks down as soon as the distance to the closest field edge is smaller than the travel distance of laterally scattered secondary electrons which, as an estimate, is equivalent to the depth of dose maximum of a percent depth-dose curve in a 10x10 cm^2 field (Wuerfel, 2013). As pointed out by Wuerfel (2013), any detector will average the dose across its sensing volume. If the dose varies across the volume of the detector, then the effect of averaging can give a different signal compared to the signal that an infinitesimally small detector would measure if placed in the centre of the large detector. This phenomenon called volume averaging effect (or just volume effect) leads to two distinct aspects (Wuerfel, 2013): an underestimation of the dose in the centre of a small field when measuring output factors (OFs) and blurring of the penumbra in profile measurements. Thus OF and penumbra measurements are two important aspects of small-field dosimetry. Although Wuerfel (2013) pointed out that the safest way to exclude the volume effect is to choose a detector which is small enough, the experimental relationship between detector and field size is yet to be established.

Based on the importance of OF measurements in small-field dosimetry (Laub and Wong, 2003), a number of studies have investigated and compared the performances of different commercially available detectors such as ion chambers, diodes and PTW natural diamond in small fields with the aim of selecting an appropriate detector (Haryanto et al., 2002; Laub and Wong, 2003; Björk et al., 2004; Barnett et al., 2005). Large deviations between OFs measured with the different detectors were reported and one reason for the observed variation

has been attributed to the volume effect of detectors in addition to the tissue-equivalence of the detector material (Haryanto et al., 2002; Laub and Wong, 2003). Although the choice of a detector for accurate dose measurements in small-fields remains a challenge, the results of most of the studies suggested that a diamond detector is the most suitable small-field dosimeter due to its excellent dosimetric properties such as its small physical size (high spatial resolution) and near-tissue equivalence (Haryanto et al., 2002; Laub and Wong, 2003; Björk et al., 2004).

The use of natural diamond detectors for dosimetry has been tested by a number of authors (Planskoy, 1980; Hoban et al., 1994; Vatnitsky and Järvinen, 1993; Laub et al., 1997, 1999; Hugtenburg et al., 2001; Björk et al., 2000, 2002, 2004; Barnett et al., 2005; Sabino et al., 2012). However, the need for daily pre-irradiation due to the presence of uncontrolled amount of impurities; dose rate dependence; high cost and long delivery times due to the scarcity of suitable stones; lengthy selection processes of diamond stones for suitable detection properties and poor reproducibility between devices are the main limitations of natural diamond detectors (Yacoot et al., 1990; Guerrero et al., 2004, 2005, 2006; Marsolat et al., 2013). In addition to its high cost compared to other solid-state detectors and being a natural resource, natural diamond detectors are also not readily accessible (Das, 2009) and hence more difficult to provide.

Due to reproducible and optimized growth conditions, synthetic diamond has been considered and intensively investigated as an alternative to natural diamond for clinical dosimetry (van der Merwe and Keddy, 1999; Benabdesselam et al., 1999; Buttar et al., 2000; Bruzzi et al., 2000; Whitehead et al., 2001; Ramkumar et al., 2001; Fidanzio et al., 2002; Bergonzo et al., 2007; Marczewska et al., 2007; Górka et al, 2008; Tranchant et al., 2008; Gervino et al., 2010; De Angelis et al., 2010; Ade et al., 2012, 2013, 2014) as the impurity levels in synthetic diamond can be controlled to tailor its radiation detection properties (Marsolat et al., 2013). However, only a few researchers such as Ciacaglioni et al. (2012) and Marsolat et al. (2013) have reported its use under small field conditions. Although these two research groups reported on the dosimetric characterization of a synthetic single crystal diamond detector in small photon beams, the influence of crystal size relative to field size was not investigated. In addition, only Marsolat et al. (2013) to date has reported the performance of a diamond detector in small beam sizes down to 0.6x0.6 cm^2.

This study investigates the relationship between detector size and field size by analysing OFs measured with synthetic diamond crystals of various types and sizes in the dosimetry of a 6 MV photon beam with small and very small fields down to 0.3x0.3 cm^2 with the aim of selecting a suitable crystal type and detector size for small-field dosimetry.

2. Materials and methods

2.1. Radiation detectors

Eight commercially available synthetic diamond crystals of various types and sizes ranging between 0.3 and 1.0 cm and thicknesses of either 0.05 or 0.1 cm were examined. These included two high-pressure, high-temperature (HPHT) samples (HP1 and HP2) and six polycrystalline CVD (chemical vapour deposition) diamond crystals of detector grade (DG) and optical grade (OG) qualities. The labels and dimensions (in mm) of the crystals are presented in Table 1. The size of a detector in this study is defined as the lateral dimension (length, width or diameter) of the sensor perpendicular to the beam direction. Due to the rectangular shape of HP1, unlike the other crystals which are square-shaped, the two different sides with sizes of 0.64 and 0.80 cm are represented as HP1a and HP1b, respectively. The opposite surfaces of each of the diamonds were metallised as reported in a previous study (Ade et al., 2012) to provide the necessary ohmic contacts for voltage biasing and acquisition of the ionization signal. A 0.03 mm^3 Dosimetry Diode E (Type T60017) of size 0.12 cm (diameter of sensor) acting as a reference detector and a 0.6 cm^3 Farmer chamber (Type 30013) of size 2.3 cm (length of sensor (air cavity)) were also used for comparative measurements.

2.2. Experimental setup and measurements

All measurements were conducted in a Perspex phantom using a 6 MV photon beam produced by a Siemens Primus linear accelerator at the Charlotte Maxeke Johannesburg Academic Hospital. Each diamond crystal was encapsulated in a probe housing as described in a previous study (Ade et al., 2012). The probe, constructed of entirely tissue-equivalent material with a Perspex body can hold diamond crystals of various dimensions up to 1.0x1.0x0.1 cm^3, has different exposure geometries[1] ('edge-on' and 'flat-on') for impinging

[1]In the 'flat-on' geometry, the incident radiation is normal to the face of the diamond wafer, which has a larger surface area but with reduced attenuation depth. In the 'edge-on' geometry (suitable for low-energy X-rays), the incident radiation is normal to a wafer edge which has a smaller surface area but with greater attenuation depth.

Table 1: Synthetic diamond crystals and their parameters

Diamond crystals	Dimensions of crystals (mm^3)	Lateral dimensions of crystals normal to beam direction (mm)	Δ values (±0.02)
HP1	6.4 x 8.0 x 1.0	HP1a: 6.4 HP1b: 8.0	0.96
HP2	3.0 x 3.0 x 1.0	3.0	1.02
DG A1	5.0 x 5.0 x 1.0	5.0	0.91
DG A2	5.0 x 5.0 x 1.0	5.0	0.87
DG A	10.0 x 10.0 x 0.5	10.0	0.91
DG B1	10.0 x 10.0 x 0.5	10.0	0.96
OG A	10.0 x 10.0 x 1.0	10.0	0.91
OG D	10.0 x 10.0 x 1.0	10.0	0.94

radiation and is compatible with commercially available electrometer systems. The probe was then placed in its customised Perspex phantom and connected to a PTW-Freiburg Unidos E electrometer system operated manually in the 'charge' mode. An applied electric field of 1000 V/cm was used. Both the diode and ion chamber were also connected to Unidos E and biased at 0 and 400 V, respectively.

As the linear response of a diamond detector with absorbed dose rate is necessary in radiotherapy (Marczewska et al., 2007), the detectors were first evaluated for their dependence on dose rate. As modelled by Fowler (1966), the ionization signal I (corrected for leakage) measured by a solid-state detector and absorbed dose rate D_r are related by:

$$I \propto D_r^{\Delta} \quad (1)$$

where Δ is the dose rate dependence parameter or linearity index that can take a range of values around unity (usually $0.5 \leq \Delta \leq 1.0$) depending on the material characteristics. In particular, for a pure crystal or when the excitation rate is so high that traps present are unimportant, $\Delta = 0.5$; if the carrier lifetime is dominated by traps with the same capture cross sections, $0.5 < \Delta < 1.0$; uniform and quasi-uniform trap distributions over a wide range of depths in the forbidden gap lead to $\Delta \approx 1$. The value of Δ may also exceed unity if traps in the crystal have differing capture cross sections (Fowler, 1966) or are distributed non-uniformly (Mohamed Abdel-Rahman et al., 2012).

The dose rate dependence of each diamond crystal was investigated by positioning the diamond probe in the Perspex phantom at a reference depth (d_{ref}) of 4.4 cm (5 cm water equivalent) below the phantom surface. The dose rate was then varied by changing the source-to-phantom surface distance (SSD) for a 10x10 cm^2 field from 82 to 118 cm since dose rate is usually adjusted by varying the SSD or the pulse repetition frequency of the machine (Hoban et al., 1994; Fidanzio et al., 2004). The average absorbed dose rates at the depth of measurement which varied between 1.0 and 3.0 Gy/min were measured with the Farmer chamber.

Measurements for OF determination were conducted for square fields with sizes ranging between 0.3x0.3 cm^2 and 10x10 cm^2 defined in a similar way as reported by Ciacaglioni et al. (2012). Each detector was placed at the d_{ref} of 4.4 cm in a Perspex phantom using a source-axis distance (SAD) of 100 cm (SSD = 95.6 cm). The machine was set to deliver 50 monitor units (corresponding to an absorbed dose of 0.5 Gy) at a dose rate of 2 Gy/min. OFs were then defined as the ratio of the charge measured at the 4.4 cm depth for a given field of interest to that at the same depth for a 10x10 cm^2 reference field. The irradiation geometry for the measurements is illustrated in Fig. 1.

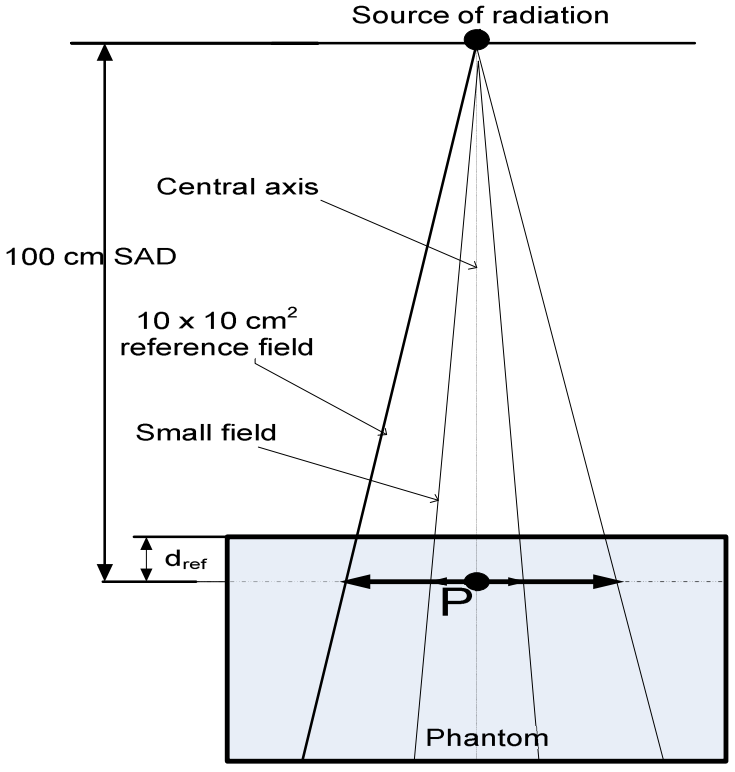

Figure 1: Irradiation geometry for OF measurements. P is the effective point of measurement of a detector and d_{ref} is the reference depth.

The sensitivity of the diamond probe for a selected crystal was also determined in a 0.5x0.5 cm^2 field and compared with the value obtained with Diode E. The sensitivity was defined as the collected charge, corrected for leakage, per unit absorbed dose and sensing volume (Górka et al., 2008).

3. Results and discussion

3.1. Dose rate dependence

The ionization signals measured with each detector as a function of absorbed dose rate were fitted by Eq. (1) using logarithmic plots to obtain the Δ values which ranged between 0.87 and 1.02 for all the diamond sensors tested in this study. The Δ values as presented in Table 1 agree with other published data (Planskoy, 1980; Ramkumar et al., 2001; Mohamed Abdel-Rahman et al., 2012). The Δ value for each detector was used to correct its response as described in Eqn. (2) below. Δ values of 1.01 and 0.99 were also obtained for the diode and ion chamber, respectively. Ion chambers are commonly used for dosimetry partly due to their near independence on dose rate (Das, 2009). It is well known that silicon diodes show strong dose rate dependence and a value of 1.20 has been reported by (Buttar et al., 2000). The large difference (17.2%) between this value and the value of 1.01 reported in this study could be related to different doping levels of Si diodes as the doping level varies for different manufacturers of diode detectors (Haryanto et al., 2002).

3.2. Output factors

Illustrated in Fig. 2 are the OFs determined for the various diamond detectors in the 'edge-on' orientation compared to measurements obtained with Diode E. Also shown are the results for the ion chamber (Fig. 2(b)). Given that OF is a factor reflecting relative dose values, the OFs for each detector were corrected for dose rate dependence using the correction factor Δ, established for each detector as follows:

$$OF = [M(d_{ref}, f)/M(d_{ref}, f_o)]^{1/\Delta} \quad (2)$$

where $M(d_{ref}, f)$ and $M(d_{ref}, f_o)$ are the charge readings obtained for a square field of size f and f_o is the reference 10x10 cm^2 field, respectively. As could be seen from Fig. 2, the OFs decrease with decreasing field size due to a decrease in scattered radiation as field size drops. As demonstrated in Fig. 2(a), the two CVD diamond crystals (DGA1 and DGA2) each of size 0.5 cm and HP1 were evaluated down to a 0.5x0.5 cm^2 field while HP2 was evaluated down to a field of 0.3x0.3 cm^2 due to its small size of 0.3 cm (Table 1). In Fig. 2(b), the 1.0 cm-size diamond crystals and ion chamber of size 2.3 cm were only assessed down to a 1x1 cm^2 field

due to their relatively large sizes. The HPHT diamonds were found to show an overall better performance compared to the CVD crystals. This could be related to the less defective nature of a HPHT diamond compared to its CVD counterparts as pointed out in two previous studies (Ade et al., 2013, 2014).

With the exception of HP2 below 0.5x0.5 cm^2 field, the differences between the OFs measured under the 'edge-on' and 'flat-on' exposure conditions for the square-shaped diamond detectors were within ±2% for field sizes down to 0.5x0.5 cm^2 as demonstrated in Fig. 3. In a previous study presented by this group using low-energy X-rays in the mammography X-ray energy range, the 'edge-on' orientation due to its greater attenuation depth was found to be about four times more absorbing than the 'flat-on' orientation (Assiamah et al., 2007). In the present study using very high-energy X-rays in the megavoltage (MV) range, the response in the 'edge-on' orientation was however found to be only about 1.02 times more than that in the 'flat-on' orientation. In other words, the variation in response between the two orientations for the diamond detectors is within ±2% which may explain why the differences between the OFs measured under the two exposure conditions is also within ±2%.

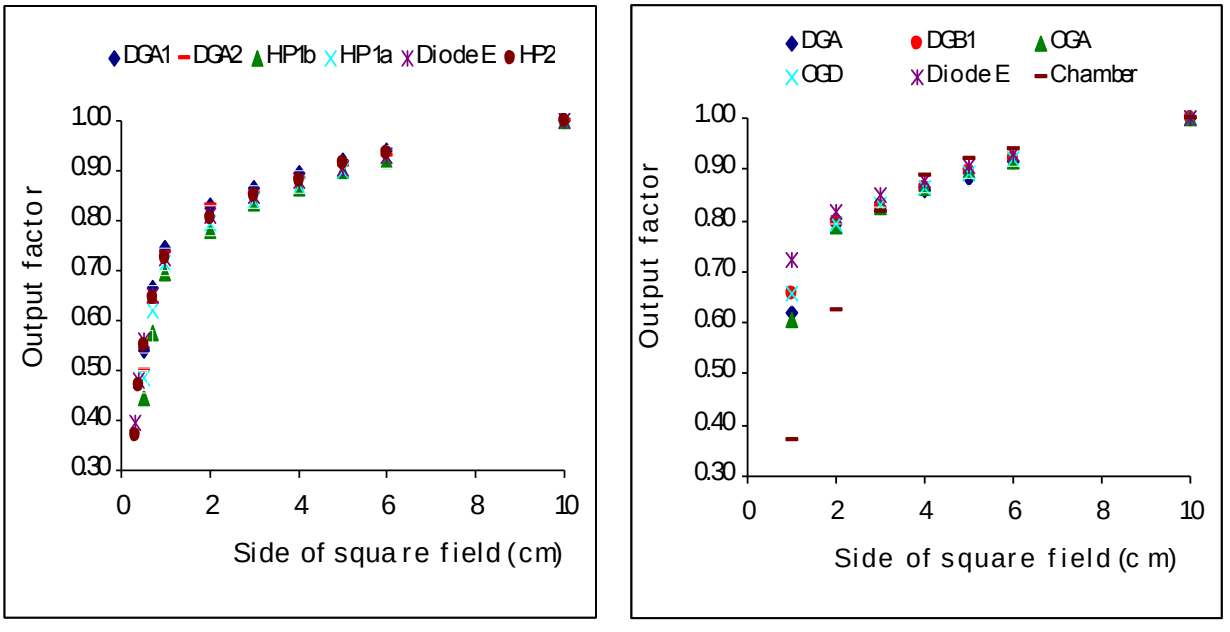

(a) (b)

Figure 2: OFs measured with (a) the HPHT and 0.5 cm-size CVD diamond detectors; and (b) the ion chamber and CVD diamond detectors of size 1.0 cm compared to measurements taken with Diode E. The figure shows only the data taken under the 'edge-on' exposure orientation for the diamond sensors.

Due to the high penetrating power of the more energetic MV X-ray photons, the small differences observed between the OFs measured under the 'edge-on' and 'flat-on' exposure conditions down to a field of 0.5x0.5 cm^2 despite a difference in attenuation depth and surface area could be attributed to the fact that the effect of the larger surface area in the 'flat-on' orientation is being compensated by the effect of greater attenuation depth in the 'edge-on' geometry. Furthermore, as the effective measuring point of the diamond probe is assumed to be its physical centre (Ade et al., 2012, 2013), the marginal difference between the two orientations for OF measurements could also be attributed to a similar effect of lateral electronic equilibrium since the distance from the centre of each diamond detector to the closest field edge is the same in both the 'edge-on' and 'flat-on' orientations. In other words, the lateral dimensions of the sensors are the same in the two exposure geometries. It is however seen that below 0.5x0.5 cm^2 field, the difference between the OFs measured under the 'edge-on' and 'flat-on' conditions for HP2 could reach 3%. The reason for this larger difference is explained later i.t.o the size/volume averaging effect of detectors in small fields.

The results presented above suggest that the performance of the detectors is greatly influenced by the maximum of the lateral or geometrical dimensions of the sensors normal to the beam direction. This hypothesis or observation is confirmed by the results of the rectangular shape crystal HP1 as displayed in Table 2. As Table 2 shows, whereas there is a

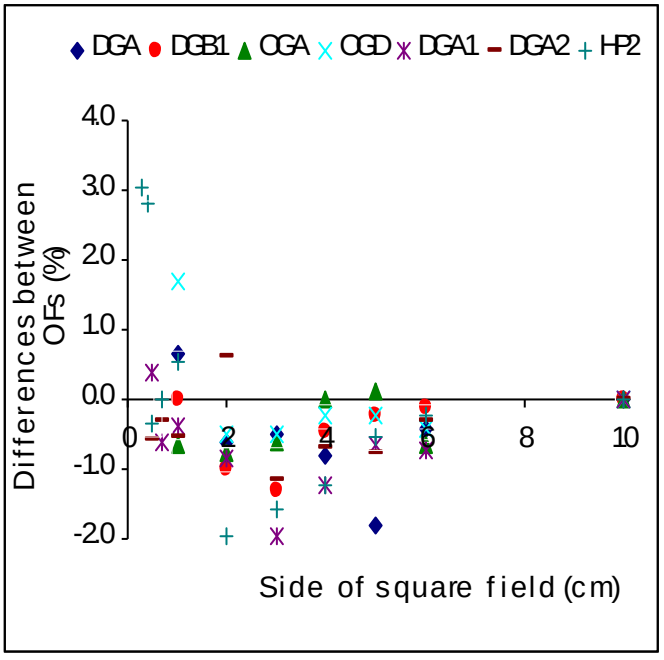

Figure 3: Percentage differences between the OFs measured under the 'flat-on' and 'edge-on'exposure conditions for the square-shaped diamond detectors.

Table 2: Percentage differences between the OFs of HP1 measured under 'flat-on' and 'edge-on' exposure conditions.

Field size (cm^2)	Percentage differences between the OFs of HP1 measured under:		
	'Flat-on' and HP1b 'edge-on' orientations	'Flat-on' and HP1a 'edge-on' orientations	HP1b and HP1a 'edge-on' orientations
6 x 6	-1.6	-0.6	0.9
5 x 5	-1.0	-0.7	0.3
4 x 4	-0.8	-0.1	0.7
3 x 3	-0.2	0.4	0.6
2 x 2	-0.3	1.3	1.1
1 x 1	0.1	3.4	3.2
0.7 x 0.7	0.5	8.4	7.9
0.5 x 0.5	1.1	9.9	8.8

small difference (≤ ±2%) between the OFs measured under 'flat-on' and HP1b 'edge-on' orientations down to a 0.5x0.5 cm^2 field, a significant difference (>3%) could be observed between the OFs measured under the 'flat-on' and HP1a 'edge-on' exposure conditions and under the two 'edge-on' orientations (HP1b and HP1a) for field sizes below 2x2 cm^2. The reason for the small differences between the OFs measured under 'flat-on' and HP1b 'edge-on' orientations is because the performance of the sensor in the 'flat-on' geometry is determined by the larger dimension which equals that for HP1b. On the other hand, the large differences observed between the OFs measured under the 'flat-on' and HP1a and under the two 'edge-on' exposure conditions below 2x2 cm^2 field size is due to a difference in the lateral dimensions of the sensor under the set conditions. In fields below 2x2 cm^2, the volume effect has a greater influence on the larger dimension.

The relative differences or dose deviations between the OFs measured with the various detectors and Diode E (reference detector) are illustrated in Fig. 4. For field sizes down to 2x2 cm^2, all the diamond detectors showed a dose deviation within ±2% while large deviations were obtained for the 1.0-cm size diamonds at 1x1 cm^2 field (Fig. 4(b)). On the other hand it could be observed that below 4x4 cm^2 field the 0.6 cm^3 Farmer chamber shows

a significant under-response with a dose deviation that is > 3% and a value of 49% was obtained for a 1x1 cm^2 field. Such a large variation is comparable to the results reported by Haryanto et al. (2002) where a difference of 35% between the OFs measured with a diode and a 0.125 cm^3 ion chamber was reported in a 1x1 cm^2 field. It should be noted that the Farmer chamber is suitable for dose measurements for field sizes ≥ 5x5 cm^2. The large dose difference could be attributed to two possible reasons - both related to the absence of lateral electronic equilibrium in small fields (Haryanto et al., 2002): detector size and tissue-equivalence of the detector. Compared to a small-size detector, a detector with a larger size would reduce the OF measured in small fields. The influence of detector size in this study is investigated in detail in section 3.3 whereas the effect of tissue equivalence has been discussed by Haryanto et al. (2002).

Detailed results for the dose deviations obtained with the rectangular-shaped diamond HP1 under the 'flat-on' and 'edge-on' exposure conditions are presented in Table 3. Compared to the HP1a 'edge-on' orientation, it could be observed from Table 3 below 3x3 cm^2 field that the dose deviations obtained under the 'flat-on' and HP1b 'edge-on' orientations are similar and larger. The smaller dose deviations obtained using HP1a compared to HP1b could be

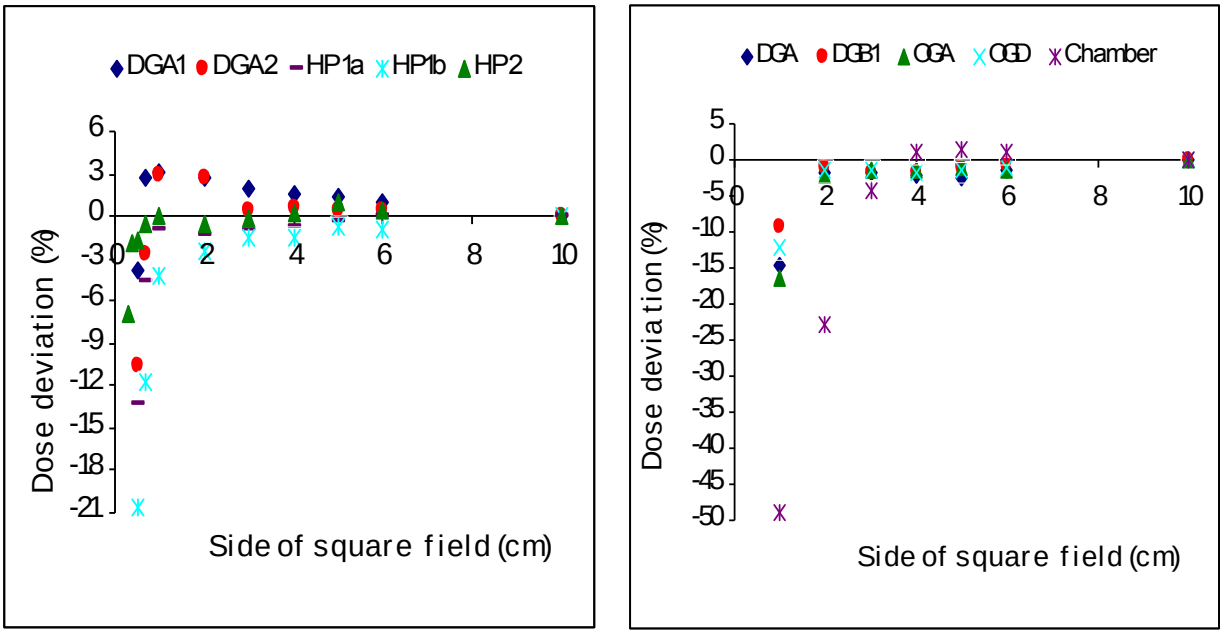

(a) (b)

Figure 4: Dose deviations (%) between the OFs measured with the various detectors illustrated in Figure 2 and Diode E: (a) the HPHT and 0.5 cm-size CVD diamond sensors; (b) Farmer chamber and 1.0 cm-size CVD diamond sensors.

Table 3: Dose deviations between the OFs measured with HP1 and Diode E for various field sizes for a 6 MV photon beam calculated as a percentage of the diode values. The table displays the results of the data taken under the 'flat-on' and 'edge-on' exposure conditions with the diamond sensor.

Field size (cm^2)	'Flat-on' Orientation	'Edge-on' Orientations	
		HP1b	HP1a
6 x 6	0.8	-0.9	0.1
5 x 5	0.2	-0.8	-0.4
4 x 4	-0.7	-1.5	-0.8
3 x 3	-1.3	-1.5	-0.9
2 x 2	-2.6	-2.5	-1.4
1 x 1	-4.3	-4.1	-1.0
0.7 x 0.7	-12.3	-11.8	-4.6
0.5 x 0.5	-21.6	-20.7	-13.4

attributed to the smaller lateral dimension of HP1a. On the other hand, the dose deviations obtained using the 'flat-on' and HP1b 'edge-on' orientations are similar because with the lateral dimensions of 0.64 and 0.80 cm, the performance of the sensor in the 'flat-on' geometry is determined by the larger dimension as mentioned earlier. With a drop in field size relative to detector size, the under-response of HP1 increases in both the 'flat-on' and 'edge-on' orientations. It could be observed that the dose deviation becomes very significant when the detector size approaches the critical point – the point where the size of the detector is comparable to the field size. Beyond the critical point, the dose deviation increases dramatically and it is likely due to the volume effect which becomes very pronounced.

Although there is a small difference between the dose deviations (or OFs) obtained under the 'flat-on' and 'edge-on' orientations, the 'flat-on' geometry seems to give a slightly larger dose difference of at about 1% especially in fields below 1x1 cm^2 (Table 3). The larger dose deviation that results from the under-response of the detector could be attributed to a greater influence of the volume effect on the 'flat-on' geometry due to its larger surface area compared to the 'edge-on'. The 'edge-on' orientation with its greater attenuation would tend to reduce the influence of the volume effect.

The above presentation suggests that the lateral dimensions, attenuation depth and surface area of the sensors are important parameters that determine the effect of detector size in small fields with the effect of lateral dimension dominating. In addition, the presented results indicate that the 'edge-on' orientation due to its greater attenuation depth and reduced surface area seems to be a preferred geometry for OF measurements especially for very small fields. For instance in addition to the results displayed in Table 3 for HP1, a maximum dose deviation of 1.9% was observed between the OFs measured with Diode E and HP2 in the 'edge-on' orientation compared to a 4.6% deviation in the 'flat-on' geometry down to a 0.4x0.4 cm^2 field. As the detector size is approaching its critical point, the larger dose deviation of 4.6% observed in the 'flat-on' orientation could be ascribed to a greater influence of the volume effect due to the larger surface area of the 'flat-on' geometry compared to the 'edge-on' orientation as explained earlier. With the same crystal HP2 in a 0.3x0.3 cm^2 field size, dose deviations of 6.4% and 9.1% were obtained under the 'edge-on' and 'flat-on' exposure conditions, respectively. Although both exposure orientations give significant dose deviations (as the detector size is already at its critical point), it is seen that compared to the 'edge-on' orientation, a larger dose difference is obtained with the 'flat-on' geometry. The results presented in Fig. 4(b) also demonstrate that the Farmer chamber with a size of 2.3 cm gives a very large dose deviation beyond its critical point (beyond a 2x2 cm^2 field).

3.3. The influence of detector size on the output factors

In order to attain the ICRU overall ±5% uncertainty of absorbed dose delivery in radiotherapy (International Atomic Energy Agency, 1997; International Commission on Radiation Units and Measurements, 1976), the American Association of Physicists in Medicine (AAPM TG 40, 1994) has set a tolerance value within 3% for the dosimetry of both electron and photon beams. For field sizes down to 2x2 cm^2, Haryanto et al. (2002) reported that the OFs measured with different detectors showed good agreement within 3%. Similar results have been obtained in this study and it was pointed out earlier that the large deviations (>3%) shown by the Farmer chamber for field sizes below 4x4 cm^2 could be related to the effect of volume averaging due to its larger size relative to field size. The effect of detector size on OF measurements is investigated and illustrated in Fig. 5 for field sizes between 0.5x0.5 cm^2 and 4x4 cm^2 using Diode E, HP1a, HP1b and HP2 which have different sizes. Fig. 5 demonstrates that for a given field, the OF (Fig. 5(a)) decreases (or the deviation between the OF measured with the HPHT diamonds and Diode E (Fig. 5(b)) increases) with increasing detector size.

The under-response of the detectors becomes very large for field sizes ≤ 1x1 cm^2. Quadratic functions were used to fit the data presented in Fig. 5. A similar trend illustrated in Fig. 5(a) has been observed by Laub and Wong (2003) for a 1x1cm^2 field after performing an experiment to verify the volume effect of detectors in small photon fields using different commercially available detectors (a diode, PTW diamond and ion chambers).

Since the measurement of OFs in small fields is affected by both detector and field sizes, the influence of detector size relative to field size was investigated by plotting the relative differences between the OFs measured with the various detectors and Diode E as a function of the ratio of detector size to field size as illustrated in Fig. 6. Only the dose deviations due to the under-response (volume effect) of the detectors are plotted using absolute values. Fig. 6(a) shows the results for the diamond detectors and Fig. 6(b) shows the data for both the diamond detectors and ion chamber. The large sizes of the detectors relative to the field size explain the dramatic change in slopes observed in Fig. 6. It is seen that as the detectors approach the critical limit (the point where the ratio of detector size to field size is unity), the dose deviation increases sharply and beyond the critical point, the under-response of the

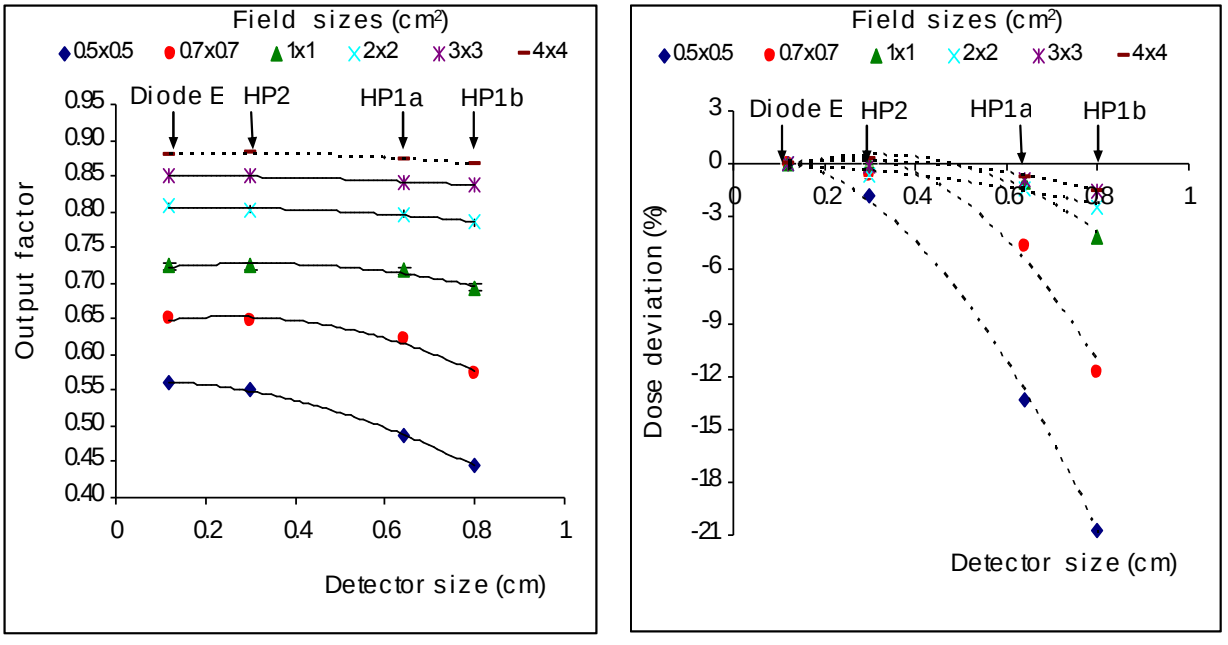

(a) (b)

Figure 5: (a) OFs as a function of detector size for the HPHT diamonds and Diode E for various field sizes represented by the different symbols. **(b)** Dose deviations (%) between the OFs measured with the HPHT diamonds and Diode E as a function of detector size for various field sizes represented by the different symbols. The data for the diamonds were taken under the 'edge-on' exposure orientation.

detectors (HP1 and ion chamber) becomes very large as mentioned earlier. It could however be observed that the slopes for the HPHT diamonds (HP1 and HP2) seem to change more slowly compared to the CVD crystals. Such an observation could be attributed to a combined process of the volume averaging effect and the difference in the material quality of a HPHT diamond compared to its CVD counterparts as pointed out in two previous studies (Ade et al., 2013; Ade et al., 2014). Firstly, at the critical point the volume effect already has a very large negative influence on the performances of the detectors. Secondly, CVD diamond crystals being polycrystalline materials have high defect densities due to their non-homogeneous structure (Bergonzo et al., 2007) compared to HPHT diamonds. In particular, it is well known that polycrystalline CVD diamond films have a high concentration of grain boundaries (Balducci et al., 2005) where electron traps are concentrated or in more defective regions (Manfredotti et al., 2006). Therefore depending on the distribution of defects, as charge carriers spread out in the course of averaging the dose across the measuring volumes of the CVD diamond sensors the presence of such defects acting as trapping centres could be a factor contributing to the sharp under-response of the CVD diamond detectors at the critical point compared to the HPHT diamond sensors.

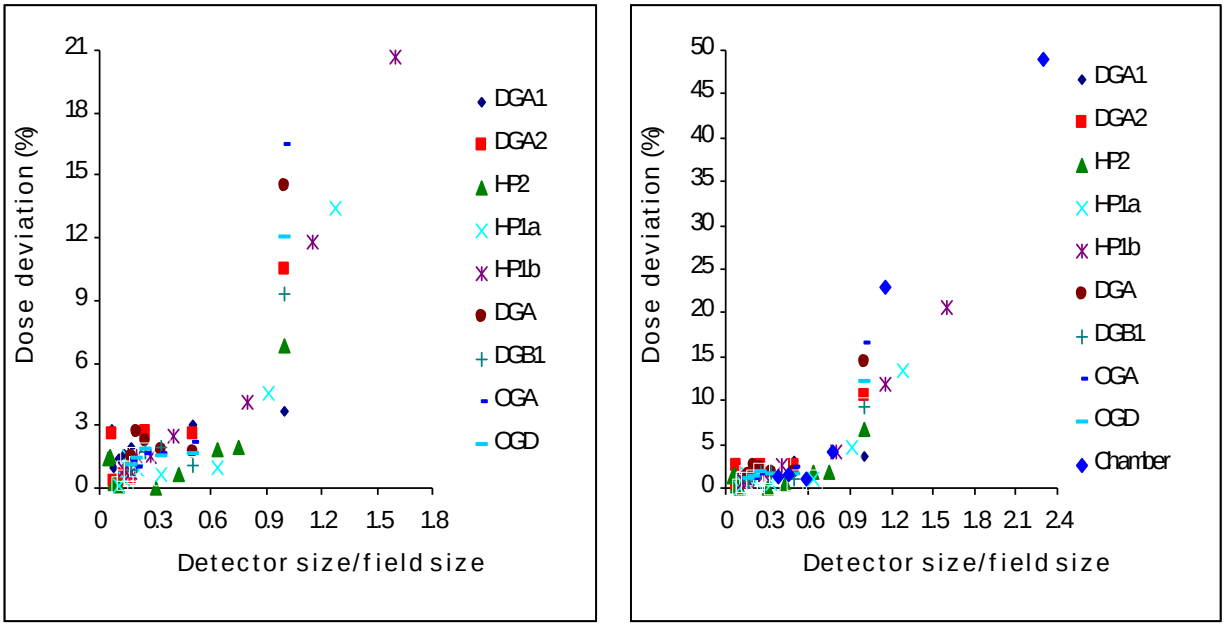

Figure 6: Dose deviations (%) between the OFs measured with the various detectors and Diode E as a function of the ratio of detector to field size for the: (a) diamond sensors and (b) diamond sensors and ion chamber. Only the absolute values of the dose deviations due to the under-response of the detectors are plotted.

It could be observed from Fig. 6(b) that with a larger ratio of detector size to field size of 1.6 for the diamond sensor HP1b compared to a value of 1.15 for the Farmer chamber, the diamond detector gives a smaller dose deviation of about 21% compared to 23% obtained with the chamber. This may demonstrate that the volume effect has a greater influence on ion chambers compared to solid-state detectors although the tissue-equivalence of diamond may also play a part. Comparisons of measurements made with different ion chambers by Haryanto et al. (2002) showed that the size of the air cavity is the key aspect for these types of detectors. Detectors with large air cavities will reduce the relative dose in small fields because the detector averages the dose across its sensing volume. In addition, the larger the size of the air cavity, the greater the effect of lateral electronic disequilibrium resulting to a lower dose for the air within the cavity compared to the case with tissue.

It can be estimated from Fig. 6 that the dose deviation is within 3% when the ratio of detector to field size is ≤ 0.75. In other words, the under-response of the detectors will be > 3% when the detector size is > 3/4 (or 75%) of the field size. This is also approximated by the slope (0.73 or 73%) of the graph in Fig. 7 which shows the relationship between field and detector size for the various detectors when the dose deviation between OFs measured with the detectors and Diode E is > 3%.

In comparison, Wuerfel (2013) formulated from a theoretical example that if the detector width is at least four times smaller than the field width, then this will result to only a 2% deviation due to the volume effect. The example assumed an ideal circular detector of 0.5 cm diameter in an ideal circular 2D Gaussian field having a 2.0 cm FWHM Guassian dose profile where the average signal over the detector area was calculated and compared to the value in the centre of the Gaussian. Based on experimental evidence presented in this study, it can be formulated as a rule of thumb that if the detector size is ≤ 3/4 of the field size, then the dose deviation will be within 3%. The large difference between the value calculated by Wuerfel (2013) and the results presented in this study might be due to a difference between theoretical and experimental conditions. Forinstance, in simulations utilising a diamond detector, a pure carbon atom (or graphite with a density of 2.26 g cm^{-3}) is usually assumed and substituted for diamond (Haryanto et al., 2002) whereas in the real case, the diamond matrix may be embedded with impurities which are usually not taken into account.

3.4. Comparison of sensitivity values

Due to its small size and good performance down to a field size of 0.4x0.4 cm^2, a sensitivity value of 197.3 nC Gy^{-1} mm^{-3} was determined in a 0.4x0.4 cm^2 field for the diamond probe using HP2 as a sensor compared to a value of 136.1 nC Gy^{-1} mm^{-3} obtained with Diode E. By virtue of the solid-state/air density ratio, which is of the order of 3.0 x 10^3 (Bruzzi et al., 2000), an advantage of using solid-state detectors is that they are more sensitive than air ion chambers.

Although impurities are well known to affect the response of a diamond detector to radiation, the higher sensitivity value obtained with the diamond probe compared to the silicon diode could be ascribed to the higher mass density of diamond (density = 3.515 g cm^{-3}) compared to a value of 2.33 g cm^{-3} for silicon (Mainwood, 2000). In other words, the ratio of the mass density of diamond to silicon is about 1.5. The results also indicate that the diamond sensor is 1.45 times more sensitive that the silicon diode. The higher sensitivity value of the diamond probe compared to the diode implies a better signal-to-noise ratio which is preferable in measurements such as profiles and percent depth-dose curves (DETECTOR). The better the SNR, the faster the measurements can be carried out. In this study, a SNR of about 1.8 x 10^4 was established for the probe using HP2 as sensor in a 10x10 cm^2 field compared to the values of 10 and 2.6 x10^3 reported for polycrystalline (Fidanzio et al., 2004) and single crystal CVD diamond detectors (Tromson et al., 2010) respectively, under the same conditions.

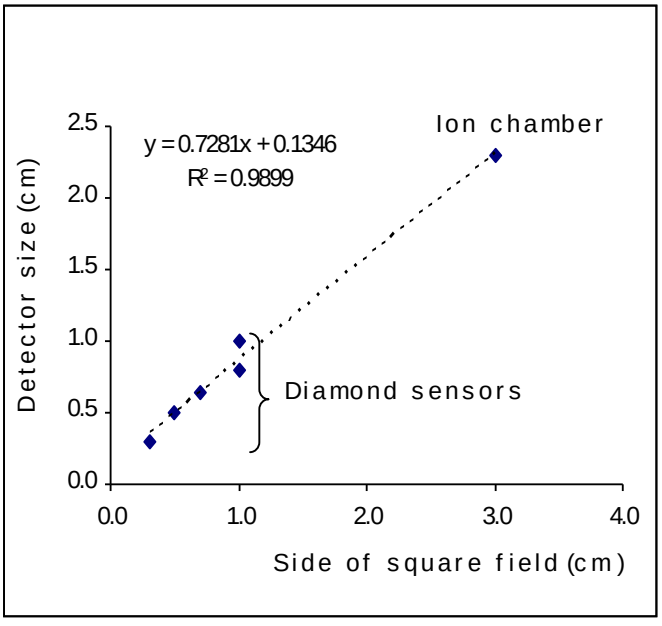

Figure 7: Relationship between field size and detector size for the detectors when the dose deviation between the OFs measured with the detectors and Diode E is > 3%.

4. Conclusions

Using synthetic diamond detectors of various types and sizes as radiation sensing elements, this study investigated the influence of detector size relative to field size in small-field photon beam dosimetry aimed at selecting a suitable crystal type and detector size for accurate dose measurements in small-fields. Based on the importance of output factor (OF) measurements in small fields, the study analysed OFs measured with various detectors for fields ranging between 0.3x0.3 cm^2 and 10x10 cm^2. Relatively large-size detectors were found to exhibit significant under-response in smaller fields and the HPHT diamonds showed an overall better performance compared to the CVD crystals with the 'edge-on' orientation being a preferred geometry for OF measurements. The results indicated also that the dose deviations between the OFs measured with the various detectors and Diode E increase with increasing detector size and it was established that the deviation would be > 3% when the detector size is > 3/4 of the field size. The results of the study further pointed out that with careful selection of a suitable crystal type of a given size and orientation the relative dose measured with the diamond probe in small fields would agree favourably within ±2% with that measured with a small-field detector but with a higher sensitivity value.

To the best of our knowledge, this is the first study that has experimentally investigated the performance of a synthetic diamond probe for very small photon fields down to 0.3x0.3 cm^2.

Acknowledgements

This project is funded by the Department of Science and Technology and National Research Foundation of South Africa. We thank the Division of Medical Physics at the Charlotte Maxeke Johannesburg Academic Hospital for granting us permission to use their medical equipment.

References

AAPM, American Association of Physicists in Medicine, AAPM TG 40, 1994. *Med. Phys.* **21**, 581.

Ade, N., Nam, T.L., Assiamah, M., 2012. *Radiat. Phys. Chem.* **81**, 232.

Ade, N., Nam, T.L., Mhlanga, S.H., 2013. *Radiat. Phys. Chem.* **86**, 42.

Ade, N., Nam, T.L., Derry, T.E., Mhlanga, S.H., 2014. *Radiat. Phys. Chem*. **98**, 155.

Assiamah, M., Nam, T.L., Keddy, R.J., 2007. *Appl. Radiat. Isot.* **65**, 545.

Balducci, A., Macro Marinelli, Milani, E., Morgada, M.E., Prestopino, G., Scoccia, M.,

Tucciarone, A., Verona-Rinati, G., 2005. *Appl. Phys. Lett.* 87, 222101.

Barnett, E., Mackenzie, M., Fallone B.G., 2005. Radiol. Oncol. **39**, 71.

Benabdesselam, M., Iacconi, P., Briand, D., Lapraz, D., Butler, J.E., 1999. *Radiat. Prot. Dosim.* **84**, 257.

Bergonzo, P., Tromson, D., Descamps, C., Hamrita, H., Mer, C., Tranchant, N., Nesladek, M., 2007. *Diamond Relat. Mater.* **16**, 1038.

Björk, P., Knöös, T., Nilsson, P., 2000. *Med. Phys.* 27, 2580.

Björk, P., Nilsson, P., Knöös, T., 2002. *Phys. Med. Biol.* 47, 239.

Björk, P., Knöös, T., Nilsson, P., 2004. *Phys. Med. Biol.* 49, 4493.

Bruzzi, M., Bucciolini, M., Cirrone, G.A.P., Cuttone, G., Mazzocchi, S., Pirollo, S., Sciortino, S., 2000. *Nucl. Instrum. Methods Phys. Res.* A **454**, 142.

Buttar, C.M., Airey, R., Conway, J., Hill, G., Ramkumar, S., Scarsbrook, G., Sussmann, R.S., Walker, S., Whitehead, A. 2000. *Diamond Relat. Mater.* **9**, 965.

Ciancaglioni, I., Marco Marinelli, Milano, E., Prestopino, G., Verona, C., Verona-Rinati, G., Consorti, R., Petrucci, A., De Notaristefani, F., 2012. *Med. Phys.* **39**, 4493.

Das I.J., Diamond detector In: Rogers, D.W.O., Cyglar JE, Clinical Dosimetry Measurements in Radiotherapy. Madison, WI: *Medical Physics Publishing*, 2009. pp. 891-912.

De Angelis, C., Bucciolini, M., Viscomi, D., Marczewska, B., Onori, S., 2010. *Nucl. Instrum. Methods Phys. Res.* A **612**, 576.

DETECTORS, PTW DETECTORS catalog. Available at www.ptw.de

Fidanzio, A., Azario, L., Venanzi, C., Pinzari, F., Piermattei, A., 2002. *Instrum. Methods Phys. Res.* A **479**, 661.

Fidanzio, A., Azario, L., Viola, P., Ascarelli, P., Capelli, E., Conte, G., Piermattei, A., 2004. *Nucl. Instrum. Methods Phys. Res.* A **524**, 115.

Fowler, J.F., 1966. Solid state electrical conductivity dosimeters. *Radiation Dosimetry.* vol. II. New York: Academic. pp 291.

Gervino, G., Marino, C., Silvestri, F., Lavagno, A., Truc, F., 2010. *Nucl. Instrum. Methods Phys. Res.* A **617**, 230.

Górka, B., Fernandez-Varea, J.M., Panettieri, V., Nilsson, B., 2008. *Nucl. Instrum. Methods Phys. Res.* A **593**, 578.

Guerrero, M.J., Tromson, D., Rebisz, M., Mer, C., Bazin, B., Bergonzo, P., 2004. *Diamond Relat. Mater.* **13**, 2046.

Guerrero, M.J., Tromson, D., Bergonzo, P., Barrett, R., 2005. *Nucl. Instrum. Methods Phys. Res.* A **552**, 105.

Guerrero, M.J., Tromson, D., Descamps, C., Bergonzo, P., 2006. *Diamond Relat. Mater.* **15**, 811.

Haryanto, F., Fippel, M., Laub, W., Dohm, O., Nüsslin, F., 2002. *Phys. Med. Biol.* **47**, N133.

Hoban, P.W., Heydarian, M., Beckham, W.A., Beddoe, A.H., 1994. *Phys. Med. Biol.* **39**, 1219.

Hugtenburg, R.P., Kristen, J., Graham, J.C., Alun H.B., 2001. Phys. Med. Biol. **46**, 2489.

International Atomic Energy Agency, Quality Assurance in Radiotherapy, *IAEA-TECDOC-989, IAEA, Vienna*, 1997.

International Commission on Radiation Units and Measurements, Determination of Absorbed dose in a Patient Irradiated by Beams of X or Gamma rays in Radiotherapy Procedures, ICRU Report 24, ICRU, Bethesda, 1976

Laub, W.U., Kaulich, T.W., Nusslin, F., 1997. Phys. Med. Biol. **24**, 535.

Laub, W.U., Kaulich, T.W., Nusslin, F., 1999. Phys. Med. Biol. **44**, 2183.

Laub, W.U., Wong, T., 2003. *Med. Phys.* **30**, 341.

Lee, S. H., Kim, J., Nam, Y. S., Cho SamJu, Kwon, S., Lee, S., Shim, J.B., Kim, C.Y., Min, C.K., Cho, K.H., Huh, HyunDo, 2012. *Journal of the Korean Physical Society*, **60**, 875.

Mainwood, A., 2000. Semicond. Sci. Technol. **15**, R55.

Manfredotti, C., Fizzotti, F., Garino, Y., 2006. *Diamond Relat. Mater.* **15**, 1362.

Marczewska, B., Kupriyanov, I., Pal'Yanov, Yu., Nowak, T., Olko, P., Rębisz, M., Waligórski, M.P.R., 2007. *Diamond Relat. Mater.* **16**, 191.

Marsolat1, F., Tromson, D., Tranchant, N., Pomorski, M., Le Roy, M., Donois, M., Moignau, F., Ostrowsky, A., De Carlan, L., Bassinet, C., Huet, C., Derreumaux, S., Chea, M., Cristina, K., Boisserie, G., Bergonzo, P., 2013. *Phys. Med. Biol.* **58**, 7647.

Mohamed Abdel-Rahman, A.E., Lohstroh, A., Jayawardena, I., Henley, S.J., 2012. *Diamond Relat. Mater.* **22**, 70.

Planskoy, B., 1980. *Phys. Med. Biol.* **25**, 519.

Ramkumar, S., Buttar, C.M., Conway, J., Whitehead, A.J., Sussman, R.S., Hill, G., Walker, S., 2001. *Nucl. Instrum. Methods Phys. Res.* A **460**, 401.

Sabino, T., Rodrigues, L.N., Furnari, L., Watanabe, E.Y., Menegussi, G., 2012. Radiol. Bras.**45**, 35.

Tranchant, N., Tromson, D., Descamps, C., Isambert, A., Hamrita, H., Bergonzo, P., Nesladek, M., 2008. *Diamond Relat. Mater*. **17**, 1297.

Tromson, D., Rebisz-Pomorska, M., Tranchant, N., Isambert, A., Moignau, F., Moussier, A., Marczewska, B., Bergonzo, P., 2010. Single crystal CVD diamond detector for high

resolution dose measurement for IMRT and novel radiation therapy needs. *Diamond Relat. Mater.* **19**, 1012

van der Merwe, D.G., Keddy, R.J., 1999. *Radiat. Phys. Chem.* **54**, 325.

Vatnisky, S., Järvinen, H., 1993. *Phys. Med. Biol.* **38**, 173.

Whitehead, A.J., Airey, R., Buttar, C.M., Conway, J., Hill, G., Ramkumar, S., et al., 2001. *Nucl. Instrum. Methods Phys. Res.* A **460**, 20.

Wuerfel, J.U., 2013. Med. Phys. Int. J. **1**, 82.

Yacoot, A., Moore, M., Makepeace, A., 1990. *Phys. Med. Biol.*, **35**, 1409.

Zhu, T.C., 2010. Journal of Physics: Conference Series **250**, 012056.